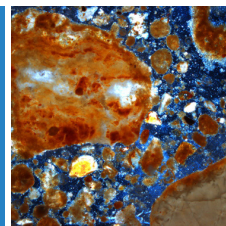


## The New HORIBA XGT-9000: An Overview



**Sofia Gaiaschi, Jocelyne Marciano**  
HORIBA FRANCE SAS, Palaiseau, France.

**Abstract:** In this technical note we present the features of the XGT-9000, the new X-ray microscope from HORIBA. We show its versatility through some examples of the application domains which could benefit from a micro X-ray fluorescence analysis.

**Keywords:**  $\mu$ -XRF; X-ray mappings, X-ray fluorescence

The **XGT-9000** is the new X-ray analytical microscope from HORIBA. The versatility of this instrument makes it a perfect tool for industrial applications, to detect failure problems or foreign particles, as well as R&D. The application domains of Energy Dispersive X-ray Fluorescence (EDXRF) range from cosmetics to pharmacy, archaeology, agro-food, metallurgy, electronics etc... Moreover, this technique can provide both qualitative and quantitative bulk composition of solid and liquid samples. In addition, when equipped with a XY table, large elemental mappings can be provided.

The principle of X-ray fluorescence is schematically represented in Figure 2. When materials are exposed to X-rays (primary X-rays in Figure 2) the ejection of one or more electrons from the inner shell of the atom may occur. The removal of an electron makes the electronic structure unstable and in order to re-establish the neutrality, electrons in the outer shells «fall» into the lower ones to fill the hole left behind. In falling, energy is released in the form of a characteristic X-ray photon, the energy of which is equal to the energy difference of the two orbitals involved ( $K\alpha$ ,  $K\beta$ ,  $L\alpha$ , etc, in Figure 2). Thus, the material emits radiation with an energy characteristic of the atoms present.



Figure 1. The new XGT-9000 microscope

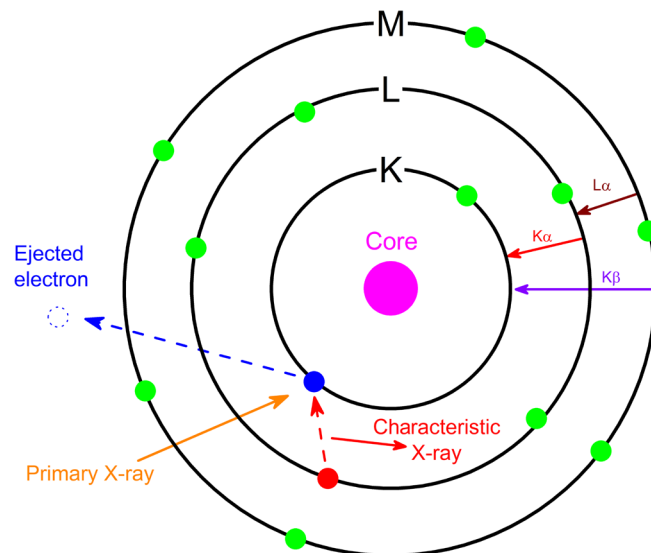


Figure 2. Schematic representation of the X-ray fluorescence phenomenon.

Figure 1 shows the standard instrument, which allows a maximum mapping size of 10x10 cm. A large chamber model (the **XGT-9000SL**) is also available, providing a maximum mapping size of 35x35 cm.

In the **XGT-9000**, the characteristic X-rays are detected thanks to an energy dispersive silicon drift detector that combines high count rate with good resolution. Furthermore, no liquid nitrogen is needed as the Peltier effect is used to cool it down.

A typical EDXRF spectrum is illustrated in Figure 3. The X-ray tube can work up to 50 kV and 1 mA. In these conditions, high energy characteristic X-Rays (e.g. Ba K $\alpha$  at 32.194 keV) can be generated, giving the possibility to deal with some interferences like Ti K $\alpha$  (4.512 keV) and Ba L $\alpha$  (4.466 keV). For instance, the high energy Ba K $\alpha$  is used for the quantification of Ba. Then, the software, using a fixed peak ratio approach, subtracts the Ba contribution from the interfering peak at ~4.5 keV, leaving just the Ti K $\alpha$  for the correct Ti quantification.

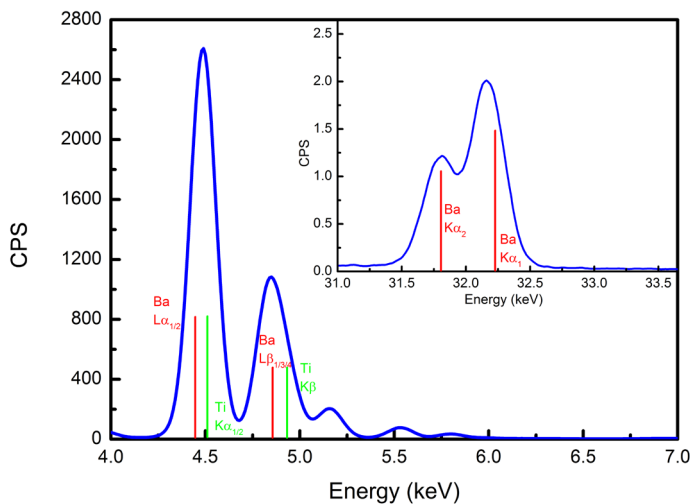


Figure 3: X-ray spectrum of barium titanate. In the inset we present the spectrum between 31 keV and 34 keV. In green we present the main Ti emission lines and in red the Ba ones. Without the high energy K $\alpha$  lines, it would be impossible to deconvolute the Ba and Ti interference in the low energy region.

The primary X-rays are focused on the sample thanks to mono or polycapillary X-Rays Guide tubes from 10  $\mu$ m up to 1.2 mm. No charging effect is induced by X-Rays irradiation, allowing to analyse the samples with little or no preparation. The system is also equipped with several energy filters, to enhance the excitation of X-rays in specific areas of the spectrum, and therefore, to identify elements at detection limits.

At a given energy, the characteristic X-Ray intensity depends on the concentration of the emitting element. However, due to interelement effects, the quantification is indirect, needing to use standard samples or the fundamental parameter method (FPM). When using standard samples, for each element to be quantified it is required to build specific calibration curves (regression between the concentration and the measured X-ray intensity, as shown in Figure 4). This method has the advantage of giving a better accuracy, however the number of calibrated elements and the calibration range depend on the available reference materials. On the other hand, the FPM is less precise, but its specificity offers the possibility to model the sample as a bulk and to calculate its composition without the need of any reference sample. Indeed, once the XRF spectrum is acquired, thanks to a suitable simulation software, equations are set up, containing expressions for primary and characteristic x-ray excitations for every element.

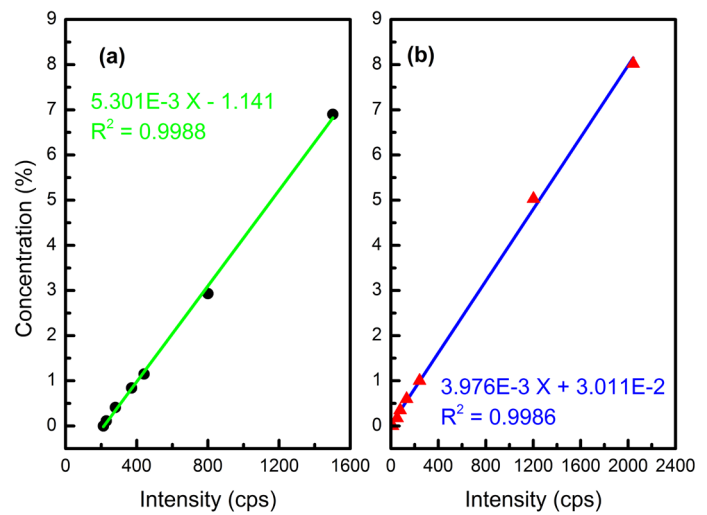


Figure 4. Examples of calibration curves for (a) Mg and (b) Si in aluminium matrix.

These complex equations also include physical and hardware fundamental parameters (e.g. x-ray absorption, incident beam energy and intensity, etc). The elemental concentration is then adjusted and compared with the actual x-ray intensities of the sample spectrum. Using an iterative process, the concentration of the sample can be calculated. The advantage of the micro-XRF is the XY table, which provides the possibility to acquire a pixel-by-pixel spectrum from which X-ray elemental images can be reconstructed, as shown in Figure 5.

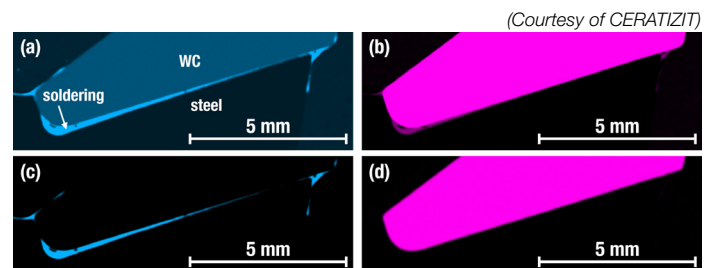


Figure 5. XRF image of circular saw blade (a) Zn raw mapping, (b) W raw mapping. Using the PS mode allows to remove the W L $\alpha$  and the Zn K $\alpha$  interference, obtaining the deconvoluted mapping (c) for Zn and (d) for W.

The software is equipped with the peak separation (PS) function, which allows the removal of interferences. Figures 5a and 5b show the raw images of Zn and W, for an SEM preparation of a circular saw blade. The blade is made mainly of steel, where WC tips are soldered using a 4900 soldering wire (Ag 49%, Cu 16%, Zn 23%, Mn 7.5% and Ni 4.5%). In the figures we see that the Zn contribution is not only detected inside the soldering, but also inside the WC; and conversely, we see a W contribution inside the soldering as well as in the WC. This is due to the overlapping of the W L $\alpha$  (8.39 keV) and the Zn K $\alpha$  (8.63 keV), as shown in Figure 6. Thanks to the PS function, pixel-by-pixel, the deconvolution of the general spectrum is performed, and the interference of these two elements are correctly removed, giving access to the final images presented in Figures 5c and 5d.

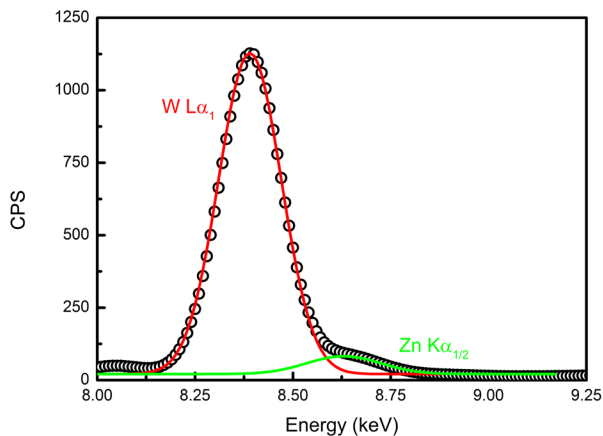


Figure 6. Zoom in on the XRF spectrum of the circular saw blade presented in Figure 5. Thanks to the PS function, the deconvolution of the  $W L\alpha_1$  and the  $Zn K\alpha$  is possible, providing the correct elemental mapping.

Furthermore, the addition of a scintillation detector placed under the sample can provide an image of X-rays transmitted. Figure 7 shows the optical image (Figure 7a), the  $Cu K\alpha$  (Figure 7b) and the X-ray transmission (Figure 7c) of an electronic component. The latter gives access to complementary information compared to those provided by the characteristic X-ray ones, showing the internal structure of the sample and therefore enabling the detection of inner details or defects.

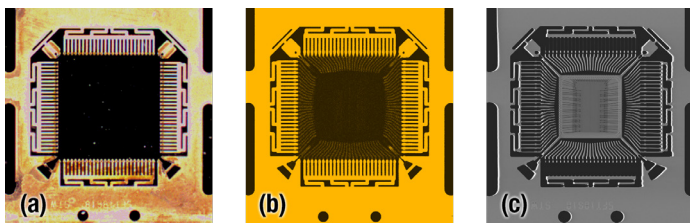


Figure 7. a) optical image, b)  $Cu K\alpha$  and c) transmission image of an electronic component.

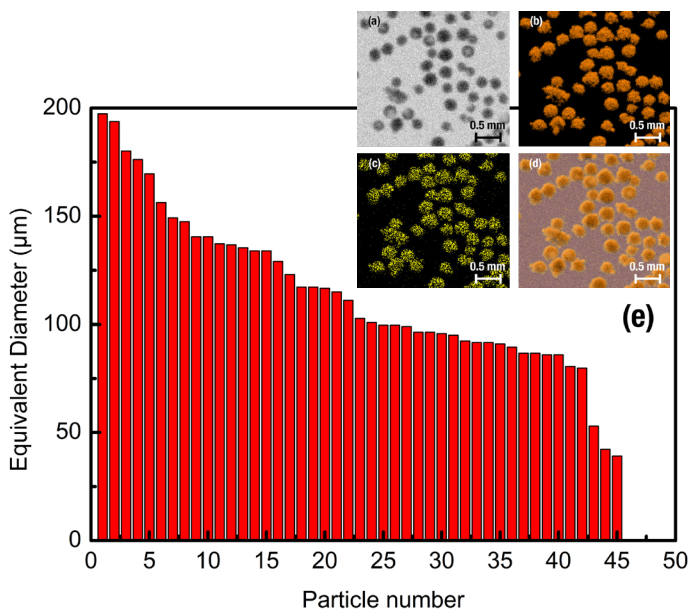


Figure 8: TiAlV particles – a) Transmitted image; b) Ti X-ray image, c) V X-ray image d) Combined image (transmitted+Ti+V) and e) Number of particles and relative size

Another feature of the **XGT-9000** software is focused on the possibility to locate and count single particles. The mappings (X-Rays, transmitted or combined, as shown in Figure 8) can be processed through this function for particle detection. Then, their average size can be measured, and a size distribution (number of particle, with its relative diameter) can be obtained. Moreover, once all the particle positions are registered, they can be used to perform point analysis on each one of them.

The instrument can be run in full or partial vacuum. The advantage of the full vacuum is the possibility to detect light elements, down to Na. However, when working in partial vacuum it is possible to analyse liquids, biological samples or hydrated ones without any damage, as they are kept at atmospheric pressure. For example, insects can be easily characterised (Figure 9).

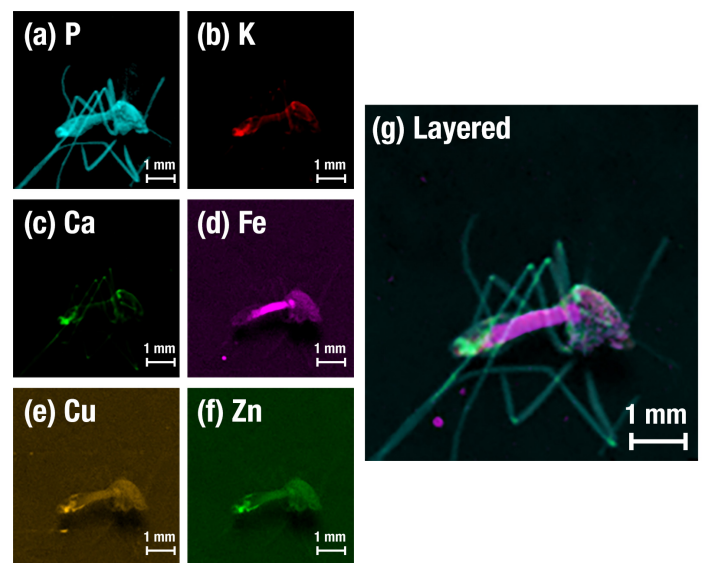


Figure 9. X-Rays mappings of a Mosquito (P, K, Ca, Fe, Cu and Zn) and combined mappings (P, K, Ca and Fe)

Finally, the micro-XRF becomes a suitable non-destructive technique for the measurement of coating thicknesses. The relatively large penetration depth of X-rays (typically from several  $\mu m$  to mm levels, depending on the analyzed matrix) allows multiple layers to be simultaneously analyzed. Therefore, with some a priori information about the elemental composition of each layer and their order, it is possible to model samples as a stack of layers. Once the XRF spectrum is acquired, the iterative process of the FPM allows to adjust and compare the simulated spectrum with the experimental one, easily providing both thickness and composition of each layer in the stack. However, the accuracy of this method is somewhat limited. For this reason, an alternative solution is to use calibration curves. As it was previously explained for the quantification, if certified thickness standards are provided, they can be used to build thickness calibration curves.